Chapter 1

Multiscale modelling of magnetic materials

Laurent Daniel[a], Laurent Bernard[b], and Olivier Hubert[c]

[a]GeePs | Group of electrical engineering - Paris (UMR CNRS 8507, CentraleSupélec, Univ. Paris-Sud, Université Paris-Saclay, Sorbonne Université) 3 rue Joliot-Curie, Plateau de Moulon 91192 Gif-sur-Yvette Cedex, France
, [b]GRUCAD/EEL/CTC, Universidade Federal de Santa Catarina, Florianópolis 88040-900, Brazil
, [c]LMT (ENS Paris-Saclay, CNRS, Université Paris-Saclay) 61 avenue du président Wilson, 94235 Cachan Cedex - France

Ferromagnetic materials are used in a wide range of applications such as sensors, actuators, motors or transformers. Their main property of interest is their capability to reach high magnetisation levels when subjected to an external magnetic field of relatively low intensity. This property originates in the complex magnetic domain microstructure and its evolution under the application of external loading. In that sense, magnetic behaviour is a very good example of multiscale phenomena, and a natural playground for multiscale modelling approaches. Of course the magnetisation curve can be described using macroscopic approaches [1], and such macroscopic approaches are necessary when it comes to numerical design of engineering parts or devices. However, because magnetic behaviour is very sensitive to many external influences - such as temperature, chemical environment, or mechanical stress - macroscopic approaches can quickly become inoperative to describe these coupled phenomena intricately related to the microstructure and its evolution. On the other hand, if the objective is to understand with more precision the formation and evolution of domain microstructures, micromagnetic approaches [2], which consider the energetic equilibrium at the scale of a set of atoms, can provide a very powerful insight into the mechanisms of ferromagnetism. Their implementation for the design of electromagnetic devices remains however most of the time out of reach.

This chapter is dedicated to multiscale approaches for the modelling of magnetic behaviour. These approaches stand between micromagnetic and macroscopic approaches. The objective is to link the basic mechanisms responsible for magnetic behaviour to the macroscopic response of ferromagnetic materials to external loadings. An emphasis will be given on the possible ways to make use of these multiscale approaches for the numerical modelling of practical engineering devices. The approach will be illustrated on applications involving

magneto-mechanical coupling effects.

1.1 MULTISCALE MODEL FOR ANHYSTERETIC MAGNETIC BEHAVIOUR OF FERROMAGNETIC MATERIALS

This section gives an overview of a multiscale modelling approach to describe the anhysteretic magnetic behaviour of ferromagnetic materials. The focus is made on the reversible part of the magnetisation process, leading to an absolute equilibrium configuration. Hysteresis will be treated in a second step as a superimposition of dissipation effects to this reversible contribution to magnetisation.

1.1.1 Energy equilibrium at the local scale

Magnetisation originates from the existence of intragranular microstructure organised in domains and separated by domain walls. At the microscopic scale, the local magnetisation $\mathbf{m} = M_s\, \alpha_i\, \mathbf{e}_i$ (with α_i the direction cosines of the magnetisation, M_s the saturation magnetisation, and using Einstein summation convention) is almost uniform in each domain and changes abruptly in the thickness of domain walls. The division into domains results from the energy balance between different elementary contributions [2]. Three contributions in particular are at the origin of this division: the exchange energy, the magnetocrystalline energy and the dipole interaction. A continuous description of the physical fields is chosen for the following developments.

The exchange energy $\mathcal{E}_{ex}$ expresses the local ferromagnetic coupling. It is described, in a medium Ω with a potential of the following form with exchange constant A:

$$\mathcal{E}_{ex} = \int_\Omega A \,\|\, \mathbf{grad}\, \mathbf{m}\|^2 \, \mathrm{d}\Omega \tag{1.1}$$

The magneto-crystalline energy $\mathcal{E}_a$ expresses the coupling between the magnetic moment orientation and crystal axes $\mathbf{d}$. This interaction is the reason for the existence of easy axes in crystalline materials and takes the form of a function $\Psi(\mathbf{d}, \mathbf{m})$. For a cubic symmetry and considering the crystal axes $\mathbf{d}$ parallel to the basis vectors $\mathbf{e}_i$, magnetocrystalline energy developed at the 6^{th} order (see chapter "Multi-scale modelling of magnetostrictive materials") is given by:

$$\mathcal{E}_a = \int_\Omega \Psi(\mathbf{d}, \mathbf{m})\, \mathrm{d}\Omega = \int_\Omega \left(K_0 + K_1(\alpha_1^2\alpha_2^2 + \alpha_2^2\alpha_3^2 + \alpha_1^2\alpha_3^2) + K_2(\alpha_1^2\alpha_2^2\alpha_3^2) \right) \mathrm{d}\Omega \tag{1.2}$$

with K_i the magneto-crystalline anisotropy constants.

The dipolar interaction plays a fundamental role in the formation of domains. It is related to the mutual interaction of the magnetic moments at position $\mathbf{r}$ with the others and to the geometry of Ω. The so-called demagnetizing field $\mathbf{H}_d(\mathbf{m})$

satisfies Maxwell equations ($\mathbf{rot}\,\mathbf{H}_d(\mathbf{m})) = \mathbf{0}$) and hence derives from a scalar potential ζ satisfying the following equations:

$$\mathbf{H}_d(\mathbf{m}) = -\,\mathbf{grad}\,\zeta \tag{1.3}$$

$$\begin{aligned} \Delta\zeta(\mathbf{r}) &= \operatorname{div}\mathbf{m}(\mathbf{r}) \;\forall\, \mathbf{r} \in \Omega \\ \Delta\zeta(\mathbf{r}) &= 0 \;\forall\, \mathbf{r} \in \mathbb{R}^3 - \Omega \end{aligned} \tag{1.4}$$

μ_0 is the vacuum permeability and ζ is the solution of a Poisson problem (1.4) and reflects the non local form of the demagnetizing field. The calculation of this quantity is usually very time-consuming. The demagnetizing energy $\mathcal{E}_d$ is usually associated to a potential of the form:

$$\mathcal{E}_d = -\frac{\mu_0}{2}\int_\Omega \mathbf{H}_d(\mathbf{m}).\mathbf{m}\;\mathrm{d}\Omega \tag{1.5}$$

The effect of the applied field $\mathbf{H}_{ext}$ on the magnetic moments is reflected by Zeeman energy $\mathcal{E}_h$:

$$\mathcal{E}_h = -\mu_0\int_\Omega \mathbf{H}_{ext}.\mathbf{m}\;\mathrm{d}\Omega \tag{1.6}$$

In addition to these terms, other contributions can be considered in the magnetic equilibrium. Mechanical effects in particular can be very significant. The mechanical contribution can partly originate from the possible application of external stress, but even in the absence of external stress, the mechanical equilibrium needs to be considered due to magnetostriction. Indeed, at a given magnetisation direction $\mathbf{m}$ is associated a free strain (eigenstrain) called magnetostriction. It is described by a second-rank tensor $\boldsymbol{\varepsilon}^\mu$. In the case of cubic symmetry, and assuming isochoric strain, $\boldsymbol{\varepsilon}^\mu$ is usually written as a quadratic form of $\mathbf{m}$ depending on two magnetostriction constants. This deformation is usually incompatible (*i.e.* not deriving from a displacement field). The elastic deformation $\boldsymbol{\varepsilon}^e$ of the magnetic medium must then accommodate this incompatibility. It results in a stress field even in absence of any external mechanical loading. The total deformation is then defined by summation of elastic and magnetostriction strain ($\boldsymbol{\varepsilon} = \boldsymbol{\varepsilon}^\mu + \boldsymbol{\varepsilon}^e$) since small perturbations assumption can usually be applied. The total deformation $\boldsymbol{\varepsilon}$ derives from a displacement field $\mathbf{u}$ (1.7) and the stress field $\boldsymbol{\sigma}$ associated to elastic deformation obeys to the equilibrium equation and constitutive law (1.8) with C the stiffness tensor of the medium.

$$\boldsymbol{\varepsilon} = \frac{1}{2}\left(\mathbf{grad}\,\mathbf{u} + {}^t\,\mathbf{grad}\,\mathbf{u}\right) = \mathbf{grad}^s\,\mathbf{u} \quad \text{in} \quad \Omega \tag{1.7}$$

$$\begin{aligned} \mathbf{div}\,\boldsymbol{\sigma} &= \mathbf{0} \quad \text{in} \quad \Omega \\ \boldsymbol{\sigma} &= C : (\boldsymbol{\varepsilon} - \boldsymbol{\varepsilon}^\mu) \quad \text{in} \quad \Omega \end{aligned} \tag{1.8}$$

The mechanical problem can also be reduced to an optimization problem where the displacement field minimises the elastic energy $\mathcal{E}_{\boldsymbol{\sigma}}$ given by the application of a variational formulation of the problem.

The elastic energy $\mathcal{E}_{\sigma}$ is defined as:

$$\mathcal{E}_{\sigma} = \int_{\Omega} \left(\frac{1}{2} \boldsymbol{\varepsilon}(\mathbf{u}) : C : \boldsymbol{\varepsilon}(\mathbf{u}) - \boldsymbol{\varepsilon}(\mathbf{u}) : C : \boldsymbol{\varepsilon}^{\mu} \right) \mathrm{d}\Omega \tag{1.9}$$

Micromagnetism is a theoretical approach to describe the process of magnetisation at a scale large enough to replace the atomic magnetic moments by continuous functions, and small enough to account for the transition zones between magnetic domains [3, 4]. The local free energy $\mathcal{E}_{tot}$ (Helmholtz) is then expressed as the sum over the volume Ω of internal and external contributions mentioned above.

$$\mathcal{E}_{tot}(\mathbf{m}, \mathbf{u}) = \mathcal{E}_h + \mathcal{E}_{ex} + \mathcal{E}_a + \mathcal{E}_d + \mathcal{E}_{\sigma} \tag{1.10}$$

The stability condition of the energy is obtained if and only if the magnetisation and displacement fields minimise the total free energy simultaneously. A condition of minimisation is the cancellation of all the partial derivatives independently. The following system needs to be solved:

$$\frac{\partial \mathcal{E}_{tot}}{\partial \mathbf{m}} = \mathbf{0} \qquad \forall\, \mathbf{x} \in \Omega \tag{1.11}$$

$$\frac{\partial \mathcal{E}_{tot}}{\partial \mathbf{u}} = \mathbf{0} \qquad \forall\, \mathbf{x} \in \Omega \tag{1.12}$$

under the constraint:

$$\|\mathbf{m}\| = M_s \; \forall \mathbf{x} \in \Omega \tag{1.13}$$

and mechanical boundary conditions (known displacements $\mathbf{u}_d$ or surface forces $\mathbf{f}_d$ at surfaces of normal $\mathbf{n}$)

$$\begin{aligned} \mathbf{u} &= \mathbf{u}_d \quad \text{in} \quad \partial\Omega_u \\ \boldsymbol{\sigma}.\mathbf{n} &= \mathbf{f}_d \quad \text{in} \quad \partial\Omega_f \end{aligned} \tag{1.14}$$

Numerical techniques such as finite element method can be used for the resolution of such a problem.

Micromagnetic approaches are very informative to understand the evolutions of domain microstructures under given magneto-mechanical loading. However the computation can be very costly, mostly due to the calculation of the demagnetising field. The element size, which has to be chosen in connection with the exchange length, representative for domain wall width can also lead to prohibitive size for the calculations. As a consequence micromagnetic computations cannot be used, to date, to describe the heterogeneous configurations in terms of materials and field distribution in practical electromagnetic systems. But they

can be helpful to build simplified models for the description of magnetic material behaviour, as will be seen in next section.

1.1.2 A model for single crystal behaviour

The previous section emphasized that the complex energetic equilibrium at the atomistic scale is the reason for the formation of the domain microstructure typical of ferromagnetic materials. If the existence of the domain microstructure is now taken as an initial assumption, simplified models can be built, following the approach of Néel phase model [5]. With the objective to describe the behaviour of single crystals, the Gibbs free energy[1] can be decomposed as the sum of the Gibbs free energy of different domains [6, 7] (see chapter "Multi-scale modelling of magnetostrictive materials" for more details). The contribution of the exchange energy, localized in domain walls, is neglected. In a single crystal, due to magneto-crystalline energy, only a limited number of orientations are encountered for the magnetisation $\mathbf{m}$. For instance, depending on the sign of the magneto-crystalline anisotropy constants, cubic materials exhibit six or eight easy magnetisation directions. A cubic crystal can then be divided into six or eight domain families α. Thus, a domain family α is treated as a region with uniform magnetisation $\mathbf{m}_\alpha$. Since magnetostriction strain is defined by the magnetisation direction, magnetostriction strain at domain scale $\boldsymbol{\varepsilon}^{\mu}_{\alpha}$ is uniform too. Magnetisation at domain scale can be written:

$$\mathbf{m}_\alpha = M_s\, \boldsymbol{\alpha} = M_s\, {}^t[\alpha_1\ \alpha_2\ \alpha_3] \tag{1.15}$$

In the case of a material with cubic crystallographic symmetry, the magnetostriction strain at domain scale is given by:

$$\boldsymbol{\varepsilon}^{\mu}_{\alpha} = \frac{3}{2}\begin{pmatrix} \lambda_{100}(\alpha_1^2 - \frac{1}{3}) & \lambda_{111}\alpha_1\alpha_2 & \lambda_{111}\alpha_1\alpha_3 \\ \lambda_{111}\alpha_1\alpha_2 & \lambda_{100}(\alpha_2^2 - \frac{1}{3}) & \lambda_{111}\alpha_2\alpha_3 \\ \lambda_{111}\alpha_1\alpha_3 & \lambda_{111}\alpha_2\alpha_3 & \lambda_{100}(\alpha_3^2 - \frac{1}{3}) \end{pmatrix} \tag{1.16}$$

where λ_{100} and λ_{111} are the saturation magnetostriction constants of the crystal along directions $< 100 >$ and $< 111 >$, respectively. Homogeneous stress and magnetic field hypotheses ($\boldsymbol{\sigma}_\alpha = \boldsymbol{\sigma}_g$ and $\mathbf{H}_\alpha = \mathbf{H}_g$)[2]. The main contributions to the Gibbs free energy of a domain family α are the magnetostatic energy $\mathcal{W}^{mag}_{\alpha}$, the magneto-crystalline anisotropy energy $\mathcal{W}^{an}_{\alpha}$, and the elastic energy $\mathcal{W}^{\sigma}_{\alpha}$. In order to consider a possible bias term, introduced for instance by residual stresses or shape anisotropy, it can be convenient to introduce a configuration energy $\mathcal{W}^{conf}_{\alpha}$ (see chapter "Multi-scale modelling of magnetostrictive materials").

1. Gibbs free energy is also defined as free enthalpy whose associated variable is stress and not deformation as for Helmholtz free energy.
2. Index α refers to the domain family scale and index g refers to the crystal scale.

The free energy $\mathcal{W}_\alpha$ of a domain family α is then uniform and written as:

$$\mathcal{W}_\alpha = \mathcal{W}_\alpha^{mag} + \mathcal{W}_\alpha^{an} + \mathcal{W}_\alpha^{\sigma} + \mathcal{W}_\alpha^{conf} \tag{1.17}$$

Due to $\mathcal{W}_\alpha^{mag}$, the magnetisation $\mathbf{m}_\alpha$ tends to align along the magnetic field $\mathbf{H}_g$ (Eq.(1.18)). μ_0 is the vacuum permeability.

$$\mathcal{W}_\alpha^{mag} = -\mu_0 \, \mathbf{H}_g . \mathbf{m}_\alpha \tag{1.18}$$

Due to $\mathcal{W}_\alpha^{an}$, the magnetisation $\mathbf{m}_\alpha$ tends to align along the easy axes. It is given by Eq.(1.19) in the case of a cubic symmetry material. K_1 and K_2 denote the magnetocrystalline anisotropy constants of the material.

$$\mathcal{W}_\alpha^{an} = K_1(\alpha_1^2\alpha_2^2 + \alpha_2^2\alpha_3^2 + \alpha_3^2\alpha_1^2) + K_2(\alpha_1^2\alpha_2^2\alpha_3^2) \tag{1.19}$$

$\mathcal{W}_\alpha^{\sigma}$ is the magnet-elastic elastic energy [6]. It can be written as a function of magnetostriction strain $\boldsymbol{\varepsilon}_\alpha^{\mu}$ and stress tensor $\boldsymbol{\sigma}_g$ (see chapter "Multi-scale modelling of magnetostrictive materials"):

$$\mathcal{W}_\alpha^{\sigma} = -\boldsymbol{\sigma}_g : \boldsymbol{\varepsilon}_\alpha^{\mu} \tag{1.20}$$

The orientation $\boldsymbol{\alpha}$ of the magnetisation in a domain family α is obtained by minimisation of the local free energy:

$$\boldsymbol{\alpha} = \underset{(\boldsymbol{\alpha} \in \mathbb{R}^3, \, \|\boldsymbol{\alpha}\|=1)}{\arg\min} \quad (\mathcal{W}_\alpha) \tag{1.21}$$

This procedure allows defining the orientation of the magnetisation in each domain family α.

Once the free energy $\mathcal{W}_\alpha$ is known for all domain families α, the volume fractions f_α of domain families α are introduced as internal variables. These internal variables can be calculated according to an explicit Boltzmann-type relation:

$$f_\alpha = \frac{\exp(-A_s \, \mathcal{W}_\alpha)}{\sum_\beta \exp(-A_s \, \mathcal{W}_\beta)} \tag{1.22}$$

where A_s is an adjustable material parameter. It can be shown [6] that A_s is proportional to the initial slope χ^o of the unstressed anhysteretic magnetisation curve:

$$A_s = \frac{3\chi^o}{\mu_0 M_s^2} \tag{1.23}$$

From the magnetisation orientation and the volume fraction of each domain family α, the magnetisation $\mathbf{M}_g$ and the magnetostriction strain $\boldsymbol{\varepsilon}_g^{\mu}$ at the single crystal scale are obtained with a volume average over the single crystal.

$$\mathbf{M}_g \; = \; \langle \mathbf{m}_\alpha \rangle_g \; = \; \sum_\alpha f_\alpha \; \mathbf{m}_\alpha \tag{1.24}$$

$$\boldsymbol{\varepsilon}_g^{\mu} \; = \; \langle \boldsymbol{\varepsilon}_\alpha^{\mu} \rangle_g \; = \; \sum_\alpha f_\alpha \; \boldsymbol{\varepsilon}_\alpha^{\mu} \tag{1.25}$$

1.1.3 Polycrystal behaviour

In order to define the behaviour of a polycrystalline material, it is necessary to assemble the behaviour of a large number of single crystals. This can be done by using a self-consistent polycrystalline scheme. The purpose is to define the local magneto-mechanical loading - local stress $\boldsymbol{\sigma}_g$ and magnetic field $\mathbf{H}_g$ - from the macroscopic magneto-mechanical loading - macroscopic stress $\boldsymbol{\sigma}_m$ and magnetic field $\mathbf{H}_m$ - using so-called localisation equations. This can be written in the general form[3]:

$$\boldsymbol{\sigma}_g = \mathcal{B}_g^{\sigma} : \boldsymbol{\sigma}_m + \mathcal{L}_g^{\sigma} : (\boldsymbol{\varepsilon}_m^{\mu} - \boldsymbol{\varepsilon}_g^{\mu}) \tag{1.26}$$

$$\mathbf{H}_g = \mathcal{A}_g^{H}.\mathbf{H}_m + \mathcal{M}_g^{H}.(\mathbf{M}_m - \mathbf{M}_g) \tag{1.27}$$

$\mathbf{M}_m$ and $\boldsymbol{\varepsilon}_m^{\mu}$ are the macroscopic (average) magnetisation and magnetostriction strain, respectively. $\mathcal{B}_g^{\sigma}$ and $\mathcal{A}_g^{H}$ are the elastic and magnetic localisation operators and $\mathcal{L}_g^{\sigma}$ and $\mathcal{M}_g^{H}$ are the elastic and magnetic incompatibility tensors defining the incompatibilities raised by the difference of behaviour between an individual grain and the surrounding medium. These tensors depend on the crystallographic orientation of the considered grain so that texture effects can be included in the modelling. The practical calculation of the localisation operators is detailed in [8, 9]. They notably depend on the elastic stiffness coefficients C_{ij} of the single crystal. Eq.(1.26) and (1.27) make use of the macroscopic magnetostriction strain $\boldsymbol{\varepsilon}_m^{\mu}$ and magnetisation $\mathbf{M}_m$ so that the scheme is self-consistent. Once the local magneto-mechanical loading $(\boldsymbol{\sigma}_g, \mathbf{H}_g)$ is known, the single crystal model is applied to obtain the strain and magnetisation at the single crystal scale. The macroscopic magnetisation $\mathbf{M}_m$ and magnetostriction strain $\boldsymbol{\varepsilon}_m^{\mu}$ are then obtained with a volume average over the polycrystal.

$$\mathbf{M}_m = \langle {}^t\mathcal{A}_g^{H}.\mathbf{M}_g \rangle_m \tag{1.28}$$

$$\boldsymbol{\varepsilon}_m^{\mu} = \langle {}^t\mathcal{B}_g^{\sigma} : \boldsymbol{\varepsilon}_g^{\mu} \rangle_m \tag{1.29}$$

The macroscopic elastic strain $\boldsymbol{\varepsilon}_m^{el}$ (obtained using the standard macroscopic Hooke law) can be added to the magnetostriction strain to obtain the total macroscopic strain $\boldsymbol{\varepsilon}_m$.

1.1.4 Summary for the multiscale modelling of anhysteretic magnetic behaviour

The modelling process can be summarised as presented in Fig.1.1.

The input data for the multiscale model (MSM) are the material parameters (including the crystallographic texture) and the applied macroscopic loading in

3. Index g refers to the crystal scale and index m refers to the polycrystal scale (Representative Volume Element).

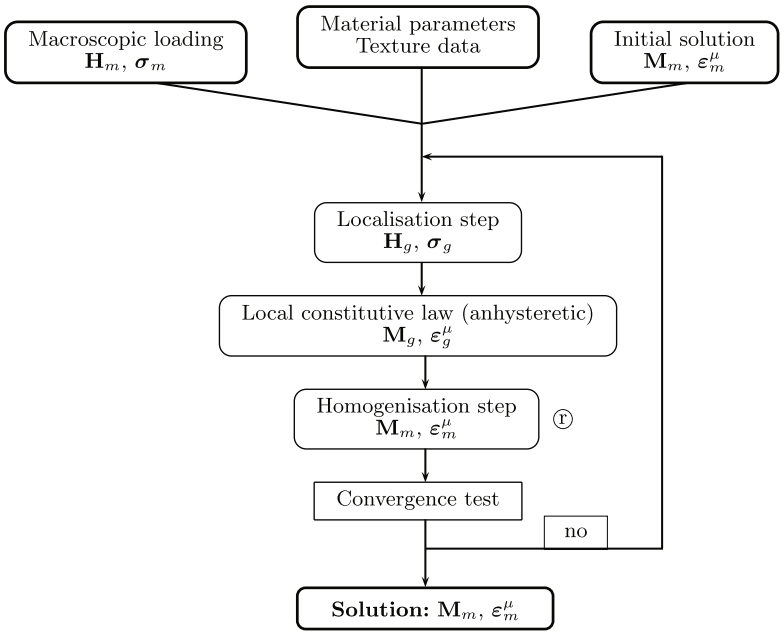


FIGURE 1.1 Calculation principle

terms of stress $\boldsymbol{\sigma}_m$ and magnetic field $\mathbf{H}_m$. An initial guess for the solution (macroscopic magnetisation $\mathbf{M}_m$ and magnetostriction strain $\boldsymbol{\varepsilon}_m^\mu$) is also needed to start the process. The use of the solution under uniform stress and uniform magnetic field assumptions is usually convenient for this initial guess. For each element of the orientation distribution function, the localisation rules (1.26) and (1.27) are applied to define the local stress $\boldsymbol{\sigma}_g$ and magnetic field $\mathbf{H}_g$. The local anhysteretic constitutive law is then applied according to the model presented in section 1.1.2 to obtain the local magnetisation $\mathbf{M}_g$ and magnetostriction strain $\boldsymbol{\varepsilon}_g^\mu$. These local responses are then averaged over the crystallographic orientations to obtain the macroscopic magnetisation $\mathbf{M}_m$ and magnetostriction $\boldsymbol{\varepsilon}_m^\mu$ (Eq.(1.28) and (1.29)). This solution replaces the initial guess, and the process is repeated until convergence. In order to ensure the convergence, a relaxation method can be used just after the homogenisation step. This process, noted by the symbol ⓣ in Fig.1.1, consists in defining the new value of $\mathbf{M}_m$ and $\boldsymbol{\varepsilon}_m^\mu$ at step k as a weighted average between the result of the homogenisation step and the previous result at step $k-1$. The final solution is given by the macroscopic magnetisation

$\mathbf{M}_m$ and the macroscopic magnetostriction strain $\boldsymbol{\varepsilon}_m^{\mu}$.

1.2 DESCRIPTION OF HYSTERESIS

The presentation has been limited so far to anhysteretic behaviour of ferromagnetic materials, which describes, for a given level of external loading, the optimal equilibrium that can be reached by the material. The magnetisation process however is associated to very significant dissipation processes that prevent the domain microstructure to reach this optimal equilibrium. These dissipation processes are mainly related to the defects in the materials and to the development of eddy currents at different scales [10]. They result in a strong hysteresis in the magnetisation process. It is important to be able to describe this hysteresis in order to model practical devices based on ferromagnetic materials. To date however, and apart from statistical approaches justifying the loss separation approach, there is no model available to accurately describe the macroscopic hysteretic response of a material from the description of the local dissipation mechanisms. This is the reason why it is often proposed to consider hysteresis in a phenomenological way, complementing the anhysteretic description of the material. These phenomenological ways should however fulfill the second law of thermodynamics (positive dissipation) to be acceptable. This point is shortly addressed in the chapter "Multi-scale modelling of magnetostrictive materials". Two approaches will be described here, the first one based on the Hauser hysteresis model, and the second one based on the Jiles-Atherton model.

1.2.1 Approach based on Hauser hysteresis model

Hauser model [11] considers that a magnetic material can be seen as a bi-domain structure: one magnetic domain along the direction of the applied field, and the other in the opposite direction. The hysteresis effect can be described by the motion of the domain wall inside this bi-domain structure. The domain wall position is defined through the use of macroscopic reduced magnetisation $\mathrm{m} = ||\mathbf{M}||/M_s$. The motion of the domain wall is represented by the variation of m. This leads to the description of an irreversible field H_{irr} as follows:

$$H_{irr} = \operatorname{sgn}(\mathrm{m} - \mathrm{m}_0)\left(\frac{k_r}{\mu_0 M_s} + c_r H_{rev}\right)\left[1 - \kappa \exp\left(-\frac{q}{\kappa}|\mathrm{m} - \mathrm{m}_0|\right)\right] \quad (1.30)$$

where q, k_r, c_r, and κ are material parameters. H_{rev} is the reversible magnetic field (used in the MSM to get the magnetisation $\mathbf{M}$). m_0 is the starting value of m at the last field reversal. The term $|\mathrm{m} - \mathrm{m}_0|$ varies from 0 to 2, describing the wall displacements from a macroscopic scale. $\operatorname{sgn}(\mathrm{m} - \mathrm{m}_0)$ is equal to $+1$ or -1 depending on the direction of the magnetic loading variation. The term k_r controls the coercivity of the hysteresis cycle. κ changes each time at the field is

reversed in order to maintain the continuity of irreversible field:

$$\kappa = 2 - \kappa_0 \left[1 - \exp\left(-\frac{q}{\kappa_0} |\mathrm{m} - \mathrm{m}_0| \right) \right] \tag{1.31}$$

where κ_0 is the recorded value of κ at the previous reversal.

Although this formulation is able to describe the hysteresis effects correctly, including remanence, coercivity and static losses, H_{irr} and H_{rev} remain unidirectional. The irreversible field is always in the direction of the reversible magnetic field. This strongly limits the use of the original Hauser model, especially for rotational field loadings. However, the bi-domain assumption in Hauser model shows a good consistence with the MSM, where a set of bi-domains can be considered in each grain (a single crystal is composed of 6 or 8 domain families depending on the sign of K_1, i.e. 3 or 4 bi-domains).

Hauser model can be adapted in order to be combined with the MSM. We consider a bi-domain β formed by a domain family α^+ and the opposite domain family α^- Following Hauser proposal, the contribution of the irreversible field of a bi-domain β can be defined as follows:

$$\mathbf{H}_{irr}^{\beta} = \mathrm{sgn}\left(\mathrm{m}^{\beta} - \mathrm{m}_0^{\beta}\right) \left(\frac{k_r}{\mu_0 M_s} + c_r H_{rev}^{\beta} \right) \left[1 - \kappa^{\beta} \exp\left(-\frac{q}{\kappa^{\beta}} |\mathrm{m}^{\beta} - \mathrm{m}_0^{\beta}| \right) \right] \boldsymbol{\gamma}^{\alpha+} \tag{1.32}$$

The reduced magnetisation m^{β}, between 0 and 1, is defined from the volume fractions of the domain families α^+ and α^-:

$$\mathrm{m}^{\beta} = \frac{f_{\alpha}^{+}}{f_{\alpha}^{+} + f_{\alpha}^{-}} \tag{1.33}$$

and k_r, q and c_r are material parameters defined uniformly within the material. m_0^{β} is the starting value of m^{β} at the previous field reversal, representing the previous position of the domain wall in the bi-domain β. $\boldsymbol{\gamma}^{\alpha+}$ is defined as the positive direction of the bi-domain β, or the direction of domain $\alpha+$. H_{rev}^{β} is the projection of local reversible field $\mathbf{H}_{rev}^{g}$ along the direction of bi-domain β ($H_{rev}^{\beta} = |\mathbf{H}_{rev}^{g}.\boldsymbol{\gamma}^{\alpha+}|$). An inversion of loading direction is defined as a change of direction of the wall motion. From a practical point of view, this inversion is detected at instant t when $\Delta\mathrm{m}_t^{\beta} \Delta\mathrm{m}_{t-1}^{\beta} < 0$. At each inversion, κ^{β} is updated to maintain the continuity of irreversible field of the bi-domain β, shown in equation (1.34). κ_0^{β} is the value of κ^{β} at the previous field inversion.

$$\kappa^{\beta} = \kappa_0^{\beta} \left[1 - \exp\left(-\frac{q}{\kappa_0^{\beta}} |\mathrm{m}^{\beta} - \mathrm{m}_0^{\beta}| \right) \right] \tag{1.34}$$

The initial value of κ^{β} controls the first magnetisation curve. Finally, the irreversible field at the grain scale is obtained by an averaging operation over all bi-domains:

$$\mathbf{H}_{irr}^{g} = \sum_{\beta} \mathbf{H}_{irr}^{\beta} f^{\beta} \tag{1.35}$$

Unlike many hysteresis models, this modelling gives a physical description of the local and global hysteresis behaviour, possessing numerous advantages. It uses local internal variable m^{β} to describe 180° domain walls motion, which is assumed to be the main physical source of hysteresis. The application of modified Hauser model for each bi-domain forms local *hysterons*, analogous to the idea of Preisach model. The volume fraction of domains oriented along different directions is given by multiscale model and material texture data. This also allows the description of material anisotropy and stress dependency. With the application of the external magnetic field, the volume fraction of the domains varies, leading to the computation of the local 180° domain walls motion, and hence hysteresis effect.
Although irreversible field $\mathbf{H}_{irr}^{\beta}$ is defined in the direction of reversible field $\mathbf{H}_{rev}^{\beta}$ and magnetisation $\mathbf{M}^{\beta}$ in each bi-domain, the macroscopic irreversible field $\mathbf{H}_{irr}$ does not necessarily lie in the direction of reversible field $\mathbf{H}_{rev}$. This forms an angular offset between the effective field $\mathbf{H}$ and reversible field $\mathbf{H}_{rev}$.

1.2.2 Approach based on Jiles-Atherton hysteresis model

The Jiles-Atherton (JA) approach [12] is another approach that can be advantageously combined with the MSM and, hence, be used to include anisotropy, texture and mechanical stress effects in the description of the behaviour of magnetic materials. The vector extension of JA model [13] is defined by the macroscopic magnetisation increment which can be expressed as

$$\mathrm{d}\mathbf{M}_{hys} = \boldsymbol{\chi}_f.\mathrm{d}\mathbf{H}_e + c\,\mathrm{d}\mathbf{M}_{an} \tag{1.36}$$

$\mathbf{H}$ is the applied magnetic field. $\mathbf{H}_e = \mathbf{H} + \alpha_{JA}\mathbf{M}_{hys}$ is the effective magnetic field which includes a contribution from the rest of the material as a fraction α_{JA} of the magnetisation. $\mathbf{M}_{an}$ represents the anhysteretic component of the magnetisation and is a function of $\mathbf{H}_e$. $\boldsymbol{\chi}_f$ is a tensor defined by:
if $\mathbf{X}_f.\mathrm{d}\mathbf{H}_e > 0$,

$$\boldsymbol{\chi}_f = \|\mathbf{X}_f\|^{-1}\mathbf{X}_f \otimes \mathbf{X}_f \tag{1.37}$$

else,

$$\boldsymbol{\chi}_f = \mathbf{0} \tag{1.38}$$

where $\mathbf{X}_f = \frac{1}{k}(\mathbf{M}_{an} - \mathbf{M}_{hys})$ and k is the so-called pinning parameter, strongly related to hysteresis losses. An explicit expression of the hysteretic differential susceptibility can be written:

$$\boldsymbol{\chi} = \frac{\mathrm{d}\mathbf{M}_{hys}}{\mathrm{d}\mathbf{H}} = \left(\boldsymbol{I} - \alpha_{JA}\left(\boldsymbol{\chi}_f + c\boldsymbol{\chi}_{an}\right)\right)^{-1}\left(\boldsymbol{\chi}_f + c\boldsymbol{\chi}_{an}\right) \tag{1.39}$$

From this, the direct JA model can be built by numerical integration. Similarly, the inverse JA model (based on the magnetic flux density) can be built from

$$\boldsymbol{\xi} = \mu_0 \frac{\mathrm{d}\mathbf{M}_{hys}}{\mathrm{d}\mathbf{B}} = \left(\boldsymbol{I} - (\alpha_{JA} - 1)\left(\boldsymbol{\chi}_f + c\boldsymbol{\chi}_{an}\right)\right)^{-1}\left(\boldsymbol{\chi}_f + c\boldsymbol{\chi}_{an}\right). \tag{1.40}$$

It can be noticed that, if c and α_{JA} are scalar, then

$$\boldsymbol{\chi}^{-1} = \left(\boldsymbol{\chi}_f + c\boldsymbol{\chi}_{an}\right)^{-1} - \alpha_{JA}\boldsymbol{I} \tag{1.41}$$

and this tensor is symmetrical if $\boldsymbol{\chi}_{an}$ is also symmetrical. This property on the differential susceptibility is not a necessary condition when hysteresis is involved but can be interesting for numerical implementation.

The anhysteretic magnetisation and differential susceptibility can be obtained from a multiscale approach instead of the Langevin function classically used in JA model. Considering the effective field $\mathbf{H}_e$ and the constant applied stress $\boldsymbol{\sigma}_0$ as input parameters for the MSM:

$$\mathbf{M}_{an} = \mathbf{M}\left(\mathbf{H}_e, \boldsymbol{\sigma}_0\right) \tag{1.42}$$

$$\boldsymbol{\chi}_{an} = \frac{\mathrm{d}\mathbf{M}}{\mathrm{d}\mathbf{H}_e}\left(\mathbf{H}_e, \boldsymbol{\sigma}_0\right) \tag{1.43}$$

The introduction of a multiscale representation of the anhysteretic behaviour in JA model allows accounting for the effect of multiaxial stress, anisotropy and texture effects on the steepness of the hysteresis loop. However, it may not be sufficient to describe the effects on the loop shape and losses. One possible solution consists in considering variations of the pinning parameter k, depending on the domain configuration given by the multiscale approach [14].

The magnetostriciton hysteresis under a constant applied stress ($\boldsymbol{\sigma}_0$) can also be calculated by defining an anhysteretic magnetic field ($\mathbf{H}_{an}$) such that:

$$\mathbf{M}_{hys}\left(\mathbf{H}, \boldsymbol{\sigma}_0\right) = \mathbf{M}\left(\mathbf{H}_{an}, \boldsymbol{\sigma}_0\right) \tag{1.44}$$

The associated magnetostriction is then given by the MSM as

$$\boldsymbol{\varepsilon}^{\mu}_{hys}(\mathbf{H}, \boldsymbol{\sigma}_0) = \boldsymbol{\varepsilon}^{\mu}(\mathbf{H}_{an}, \boldsymbol{\sigma}_0) \tag{1.45}$$

Dropping the constant parameter $\boldsymbol{\sigma}_0$ in equation (1.44), the differential of the magnetisation is:

$$\mathrm{d}\mathbf{M}_{hys}\left(\mathbf{H}\right) = \frac{\mathrm{d}\mathbf{M}}{\mathrm{d}\mathbf{H}_{an}}\left(\mathbf{H}_{an}\right).d\mathbf{H}_{an}\left(\mathbf{H}\right) \tag{1.46}$$

In this equation $\frac{\mathrm{d}\mathbf{M}}{\mathrm{d}\mathbf{H}_{an}}\left(\mathbf{H}_{an}\right) = \boldsymbol{\chi}_{an}$ is the anhysteretic differential susceptibility calculated from the MSM at the current value of $\mathbf{H}_{an}$. $\mathbf{H}_{an}$ can then be obtained by integration of

$$\mathrm{d}\mathbf{H}_{an} = \boldsymbol{\chi}^{-1}_{an}.\mathrm{d}\mathbf{M}_{hys}. \tag{1.47}$$

This approach (multiscale with JA model) results in a relatively light hysteresis model. In particular, using simplified multiscale approaches, this kind of model can be used for numerical device simulation (see sections 1.4 and 1.6).

1.3 COMBINATION OF MULTISCALE ANHYSTERETIC APPROACH AND HYSTERESIS MODELS

The anhysteretic multiscale approach presented in this section allows describing naturally the effect of crystallographic texture by introducing grain orientations. It also allows describing the effects of a multiaxial applied stress. The hysteresis models can then be combined with the anhysteretic modelling, either at the single crystal scale or, in a macroscopic way, at the polycrystal scale. It is usually necessary to incorporate the effect of stress on the hysteresis contribution since, for most materials, dissipation is also affected by stress. It is notably seen in the effect of stress on the coercive field of ferromagnetic materials. Such a combination of anhysteretic multiscale approach and hysteresis contribution provides a powerful tool to predict the behaviour of ferromagnetic materials under various external loadings, with limited input data.

However when structural analysis needs to be performed, the practical implementation of such an approach into a numerical calculation can be cumbersome. In that context, it is necessary to develop methodologies in order to apply the multiscale approach on complex structures while maintaining its main physical features. In the next section, a few simplification strategies will be presented.

1.4 POSSIBLE SIMPLIFICATIONS FOR NUMERICAL MODELLING

1.4.1 Simplification for the definition of the magnetisation orientation

At the single crystal scale, the minimisation (1.21) of the Gibbs free energy to obtain the magnetisation orientation in a domain family α can be a costly process. Instead of performing this minimisation, the space of all possible magnetisation orientations can be discretized (considering a mesh of the unit sphere) which defines a set of domain families on which the Gibbs free energy can be evaluated. Instead of considering only domains along (or close to) easy axes, all directions are considered. The volume fraction can then be evaluated on this mesh using the same formula (1.22). The volume fraction will naturally be higher in the directions with lower energy. Using this method a minimisation on 6 or 8 orientations is replaced by the evaluation of the volume fraction on the mesh of the unit sphere. The process to evaluate the magnetisation and magnetostriction at the single crystal scale is then unchanged. In order to avoid bias anisotropy effects due to a coarse mesh of the unit sphere, the set of orientations should be as dense and uniform as possible. To this purpose the nodes of an icosphere can be used (Fig. 1.2). An icosphere is a triangular mesh of the sphere built by regular subdivision of the triangular faces of an icosahedron. The set density is then determined by the icosphere order (number of subdivisions) and presents a central symmetry which ensures the existence of opposite orientation domain families and hence zero magnetisation and magnetostriction when no magnetic

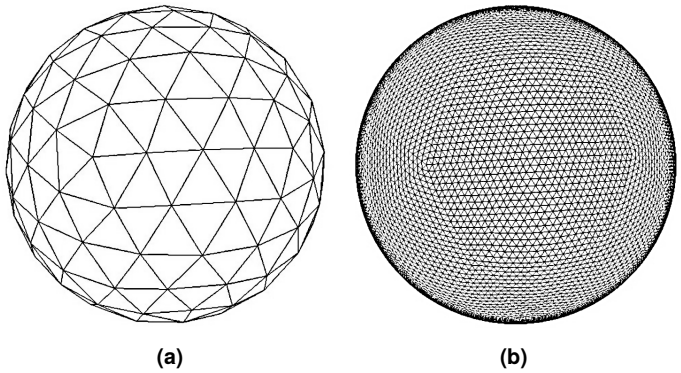


FIGURE 1.2 Icospheres with (a) 162 and (b) 10242 nodes.

field or stress is applied.

1.4.2 Uniform stress and magnetic field assumption

Another computational complexity lies at the polycrystal scale when using the self-consistent scheme to define localisation operations. This process involves an iterative evaluation of the behaviour until convergence, as illustrated in figure 1.1. A classical simplification is to neglect the fluctuations of stress and magnetic field within the material. This means that stress and magnetic field are treated as uniform:

$$\mathbf{H} = \mathbf{H}_g = \mathbf{H}_m \quad \text{and} \quad \boldsymbol{\sigma} = \boldsymbol{\sigma}_g = \boldsymbol{\sigma}_m \tag{1.48}$$

This is equivalent to neglect a part of grain to grain interactions in the modelling. While the main features of the model will be maintained, the quantitative predictions can be altered by such an assumption.

1.4.3 Macroscopically equivalent simplified texture

Another assumption can deal with the crystallographic texture of the material. A typical number of 500 different orientations as input for the MSM is needed to describe the crystallographic texture of a non-oriented electrical steel. It is possible to reduce this number by the use of equivalent simplified crystallographic textures. It is usually possible to find a set of one or two fibre textures that describes the measured texture of the material from a macroscopic perspective.

As an example, the anhysteretic magneto-elastic behaviour of a non-oriented Fe-3%Si laminated material [15] is modelled using this approach. The measured texture data are presented as pole figures (Fig. 1.3). This texture is reasonably similar to the one of a perfect $< 111 >$ fibre with its axis perpendicular to the sheet plane (Fig. 1.4). Such a texture can be obtained (for modelling) starting from a crystal with a $< 111 >$ direction perpendicular to the sheet plane and

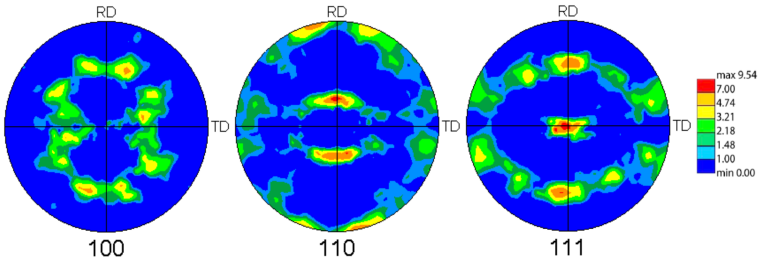


FIGURE 1.3 Pole figures (stereographic projection) for non-oriented Fe-3%Si.

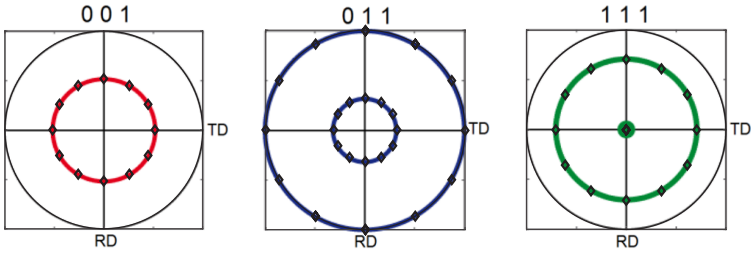


FIGURE 1.4 Pole figures for a perfect <111> fibre with the axis perpendicular to the sheet plane from [16].

generating a set of crystals by rotations, with respect to this axis, of angles uniformly distributed between 0 and $2\pi/3$ (because of the periodicity of this configuration).

A simplified fibre made of only 4 crystals, in equal proportion, which pole figures are presented in Fig. 1.4 by rhombi dots, is analysed here. The model parameters and their values are given in Table 1.1. In the simplified approach, an optimization of these parameters could be done within a reasonable range and could help in fitting with experimental results. However, the model is also able to reproduce the main characteristics of the material behaviour without such adjustments, using a small set of tabulated values.

TABLE 1.1 Parameters for Fe-3%Si from [16].

Parameter	A_s	M_s	λ_{100}	λ_{111}	K_1	K_2
Unit	m^3/J	A/m	ppm	ppm	kJ/m^3	kJ/m^3
Value	$3{\cdot}10^{-3}$	$1.6 \cdot 10^6$	23	-4.5	38	0

As an illustration, the effect of uniaxial stress (parallel to the magnetic field) on the magneto-elastic behaviour is presented in figures 1.5, 1.6 and 1.7: results from the model are on the left, experimental data from [15] are on the right

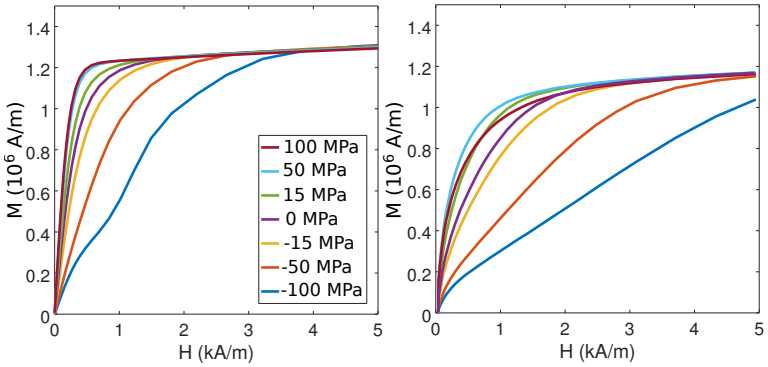


FIGURE 1.5 magnetisation as a function of the magnetic field, for different values of the uniaxial stress: MSM with simplified texture (left) from [16], measurements (right) from [15].

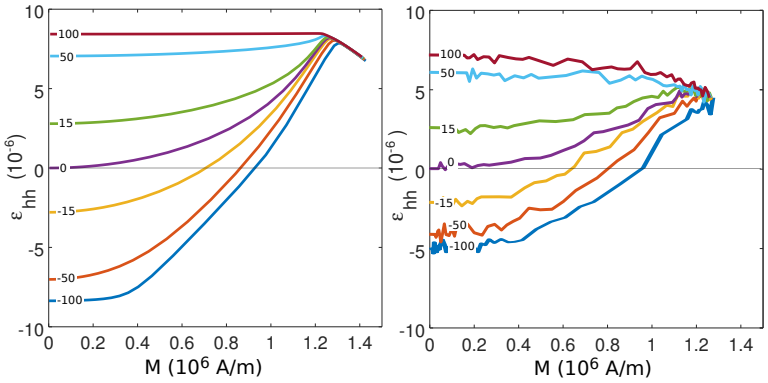


FIGURE 1.6 Parallel magnetostriction (ϵ_{hh}) in the sheet plane as a function of magnetisation, for different values of the uniaxial stress (in MPa): MSM with simplified texture (left) from [16], measurements (right) from [15].

(Magnetostriction curves are plotted using the saturation value as reference). The model reproduces the inflexion of the magnetisation curve which can be observed under strong compressive stress (−100 MPa). The change of sign of the slope of magnetostriction curves observed when reaching saturation is also represented by the model and results from magnetisation rotation.

1.4.4 Equivalent single crystal model

Further simplification for the multiscale approach consists in diluting the poly-crystalline nature of the material and considering it as a single - equivalent - crystal. In other words the material is considered as a collection of magnetic domains, independently of the grain structure.

Strongly textured materials (e.g. Goss texture materials) can be naturally

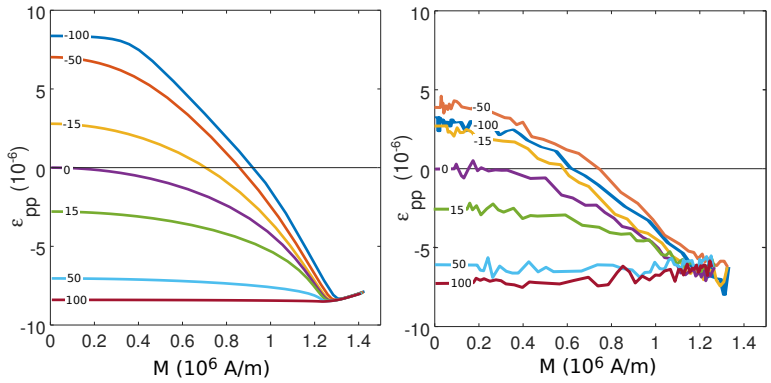


FIGURE 1.7 Perpendicular magnetostriction (ϵ_{pp}) in the sheet plane as a function of magnetisation, for different values of the uniaxial stress (in MPa): MSM with simplified texture (left) from [16], measurements (right) from [15].

treated as single crystal, and can be represented by this kind of simplified MSM [17]. Magnetostriction anisotropic tensor and anisotropy energy of the crystal can be used as a basis for the macroscopically equivalent single crystal. Some corrections can be applied in order to get a better representation of the macroscopic behaviour, in particular if structure induced anisotropy has to be accounted for (demagnetizing field effects, see chapter "Multi-scale modelling of magnetostrictive materials").

Weakly textured materials can also be treated considering this approach. The material is considered as a collection of magnetic domains, represented by a single crystal with a large number of easy directions. The local magnetostriction tensor is considered as isotropic ($\lambda_{100} = \lambda_{111} = \lambda_s$) and the anisotropy energy is adjusted in order to fit the macroscopic behaviour. The choice of an isotropic magnetostriction tensor implies that the material exhibits the same saturation magnetostriction for all directions. The macroscopic anisotropy might come from texture or structure effects. It can take different forms, e.g., $K(\boldsymbol{\alpha}.\boldsymbol{\beta})^2$ for a uniaxial anisotropy where $\boldsymbol{\beta}$ is the anisotropy direction and K is the anisotropy constant, or $K\boldsymbol{\alpha}.(\boldsymbol{N}\boldsymbol{\alpha})$ for a multiaxial anisotropy where $\boldsymbol{N}$ is a normalized diagonal matrix (in the coordinate system associated with the principal anisotropy axes). In this approach, because magnetocrystalline anisotropy is not considered as such, the effects of domain rotations are not represented and the magnetisation process can be interpreted in terms of domain wall motion only. In particular, inflexions of the magnetisation curve or changes of the slope sign of magnetostriction curve at saturation are not represented.

Another way of simplification is to consider a polycrystalline material as an anisotropic single crystal loaded in a specific crystallographic direction. This specific direction has then to be defined for each given macroscopic loading configuration.

1.4.5 Analytical model

By applying the equivalent single crystal approach and restricting the set of possible domain orientations to 6, analytical expressions for the macroscopic magnetisation and strain can be found:

$$\mathbf{M} = \frac{A_h sinh\,(\kappa H)}{A_h cosh\,(\kappa H) + A_p + A_z} M_s \mathbf{h} \tag{1.49}$$

$$\boldsymbol{\varepsilon}^{\mu} = \lambda \left(\mathbf{h} \otimes \mathbf{h} - \frac{1}{2} \left(\mathbf{p} \otimes \mathbf{p} + \mathbf{z} \otimes \mathbf{z} \right) \right) \tag{1.50}$$

with

$$\lambda = \lambda_s \left(1 - \frac{3}{2} \frac{A_p + A_z}{A_h cosh\,(\kappa H) + A_p + A_z} \right) \tag{1.51}$$

and

$$A_i = \exp\left(\tau \sigma_{ii}\right) \tag{1.52}$$

for $i \in \{h, p, z\}$, where σ_{ii} is the ii-component of the applied stress tensor. The unit vector $\mathbf{h}$ represents the direction of the magnetic field, $\mathbf{z}$ is an arbitrary unit vector perpendicular to the magnetic field and $\mathbf{p} = \mathbf{z} \times \mathbf{h}$ completes the basis. Two constants are defined as $\kappa = \mu_0 A_s M_s$ and $\tau = (3/2) A_s \lambda_s$. The analytical model offers simple expressions for the magneto-elastic behaviour and retains the effects of multiaxial stress (normal stresses with respect to the chosen basis). The variation of domain volume fractions with the magnetic field can be interpreted as a consequence of domain wall motion only. No domain rotation effect can be represented since crystal anisotropy is not considered. The effect of shear stress with respect to the chosen basis cannot be modelled either. The model does not incorporate intrinsic anisotropy, and magnetisation and magnetostriction always follow the magnetic field orientation. However induced anisotropy is accounted for as the behaviour depends on the relative orientation of the magnetic field and mechanical stress tensor.

1.5 PRACTICAL IMPLEMENTATION INTO NUMERICAL FINITE ELEMENT TOOLS

Multiscale approaches provide fully multiaxial magnetoelastic modelling: the state variables are the magnetic field vector and the mechanical stress tensor and the outputs are the magnetisation vector and the magnetostriction tensor. This multiaxiality makes it very attractive for use in field analysis and device simulations where the variety of magnetomechanical loadings is high and where uniaxial models or lookup tables are not sufficient to represent the material behaviour. However, the use of constitutive models based on multiscale approaches faces some difficulties related to the high computational cost of the numerical evaluation and the choice of state variables for the nonlinear problem resolution.

Nonlinear problem resolution methods such as the Newton-Raphson method or the modified fixed point method require the use of the same state variables for the material behaviour model and for the field analysis model. The natural state variables of multiscale models are the magnetic field and the mechanical stress. Unfortunately, usual formulations for the field analysis problems are based on the magnetic flux density (or magnetic vector potential) and on mechanical strain (or displacement) and then need an inverse material behaviour model. The inversion of multiscale models may be done numerically applying an inner Newton-Raphson procedure. However, the calculation of derivatives and the iteration process contribute to the increase of the computational cost. As a consequence, it may be interesting to choose less classical formulations based on the magnetic field (or magnetic scalar potential) and the stress together with a direct multiscale model. For both direct and inverse approaches, it is often necessary to apply some simplifying assumptions for the MSM in order to reduce computational costs. These assumptions lead to a variety of simplified multiscale models, as presented in section 1.4, the complexity and physical representativeness of which can be adapted to a particular field analysis problem.

In this section, weak formulations are presented for fully or partially coupled magnetomechanical static problems in order to show how the magnetoelastic behaviour of ferromagnetic materials is incorporated. Some details are also given on the integration, derivation and inversion of simplified multiscale models.

1.5.1 Weak formulations for field analysis

The weak formulation for magnetostatics in terms of magnetic vector potential $\mathbf{A}$ (such that the magnetic flux density is $\mathbf{B} = \mathbf{rot}\,\mathbf{A}$) can be written as:

$$\int_{\Omega_{mag}} \mathbf{H}.\,\mathbf{rot}\,\mathbf{A}'\mathrm{d}\Omega + \int_{\Gamma_{\mathbf{H}}} (\mathbf{n}\times\mathbf{H}).\mathbf{A}'\mathrm{d}\Gamma = \int_{\Omega_{mag}} \mathbf{J}.\mathbf{A}'\mathrm{d}\Omega$$
$$\forall \mathbf{A}' \in \mathcal{H}\left(\mathbf{rot}, \Omega_{mag}\right) = \{\mathbf{A}' \in \mathcal{L}^2\left(\Omega_{mag}\right), \mathbf{rot}\,\mathbf{A}' \in \mathcal{L}^2\left(\Omega_{mag}\right), \mathbf{n}\times\mathbf{A}'|_{\Gamma_{\mathbf{A}}} = \mathbf{0}\} \tag{1.53}$$

Ω_{mag} is the considered domain with complementary boundaries $\Gamma_{\mathbf{H}}$ (for Neumann conditions) and $\Gamma_{\mathbf{A}}$ (for Dirichlet conditions), and $\mathbf{J}$ is the conduction current density. $\mathbf{A}'$ is a test function that belongs to the Hilbert space $\mathcal{H}\left(\mathbf{rot}, \Omega_{mag}\right)$ and $\mathcal{L}^2(\Omega)$ is the space of square integrable vector functions on Ω_{mag}. The magnetoelastic coupling enters this formulation through the constitutive law $\mathbf{H} = \frac{1}{\mu_0}\mathbf{B} - \mathbf{M}(\mathbf{B}, \boldsymbol{\varepsilon})$.

The static elasticity formulation, considering small strains, can be written in

terms of displacement $\mathbf{u}$ (such that the total strain is $\boldsymbol{\varepsilon} = \mathbf{grad}^s\,\mathbf{u}$) as:

$$\begin{aligned}\int_{\Omega_{mec}} (C :\ \mathbf{grad}^s\,\mathbf{u}) :\ \mathbf{grad}^s\,\mathbf{u}'\mathrm{d}\Omega + \int_{\Omega_{mec}} (\boldsymbol{\sigma}_M - C : \boldsymbol{\varepsilon}^\mu) :\ \mathbf{grad}^s\,\mathbf{u}'\mathrm{d}\Omega \\ - \int_{\Gamma_\sigma} (\boldsymbol{\sigma}\mathbf{n}) \,.\mathbf{u}'\mathrm{d}\Gamma - \int_{\Gamma_{mec}} [\boldsymbol{\sigma}_M\mathbf{n}] \,.\mathbf{u}'\mathrm{d}\Gamma \\ = \int_{\Omega_{mec}} \mathbf{f}_{ext}\,.\mathbf{u}'\mathrm{d}\Omega \\ \forall \mathbf{u}', u_i' \in \mathcal{H}\,(\,\mathbf{grad}\,,\Omega) = \{u_i' \in \mathcal{L}^2\,(\Omega)\,,\ \mathbf{grad}\,u_i' \in \mathcal{L}^2\,(\Omega)\,, u_i'|_{\Gamma_\epsilon} = 0\}\end{aligned} \quad (1.54)$$

Ω_{mec} is the considered domain with complementary boundaries Γ_σ (for Neumann conditions) and $\Gamma_{\mathbf{u}}$ (for Dirichlet conditions), $\mathbf{f}_{ext}$ is the eventual external force density (of non magnetic origin), and C is the fourth-rank stiffness tensor. $\mathbf{u}'$ is a test function the components (u_i') of which belong to the Hilbert space $\mathcal{H}\,(\,\mathbf{grad}\,,\Omega_{mec})$. $\boldsymbol{\sigma}_M$ is a Maxwell tensor such that $\mathbf{div}\,\boldsymbol{\sigma}_M$ is the local magnetic force density (including Laplace forces on conduction currents and forces on magnetic material). If hysteresis is neglected, the following symmetric Maxwell tensor can be used [18]:

$$\boldsymbol{\sigma}_M = \frac{1}{2}\,(\mathbf{H}\otimes\mathbf{B} + \mathbf{B}\otimes\mathbf{H}) - w_{co}\boldsymbol{I} \quad (1.55)$$

where $\otimes$ is the tensor product (or dyadic product here), $w_{co} = \int_0^{\mathbf{H}} \mathbf{B}.\mathrm{d}\mathbf{h}$ is the magnetic co-energy density, and $\boldsymbol{I}$ is the second rank identity tensor. A surface magnetic force density might need to be accounted for on the boundary Γ_{mec} where a discontinuity $[\boldsymbol{\sigma}_M\mathbf{n}]$ exists. The surface force term can be avoided, in the weak formulation, by including an air layer around the considered solid. Magnetostriction $\boldsymbol{\varepsilon}^\mu\,(\mathbf{B},\boldsymbol{\varepsilon})$ enters the formulation through the total strain expression $\boldsymbol{\varepsilon} = \boldsymbol{\varepsilon}^e + \boldsymbol{\varepsilon}^\mu$, where $\boldsymbol{\varepsilon}^e$ is the elastic strain such that $\boldsymbol{\sigma} = C : \boldsymbol{\varepsilon}^e$.

The weak formulation for magnetostatics based on the scalar potential (ϕ) is less popular than the one based on the vector potential. In three-dimensional finite element problems, nodal elements can be used for the scalar potential which may reduce the size of the system compared to the one obtained with edge elements and vector potential. However the representation of conduction currents $\mathbf{J}$ is made more difficult because it requires the determination of a vector field $\mathbf{T}$ such that $\mathbf{J} = \mathbf{rot}\,\mathbf{T}$. Scalar potential formulations may also suffer some numerical difficulties in systems with airgaps, where strong variations of the potential are concentrated in a small region. Despite these difficulties, these formulations can be interesting in a magnetoelastic coupling context because they avoid the inversion of the material constitutive behaviour. The weak formulation

can be written as:

$$\int_{\Omega_{mag}} \mathbf{B}.\,\mathbf{grad}\,\phi' \mathrm{d}\Omega - \int_{\Gamma_{\mathbf{B}}} \mathbf{B}.\mathbf{n}\,\phi' \mathrm{d}\Gamma = 0$$
$$\forall \phi' \in \mathcal{H}\left(\mathbf{grad}, \Omega_{mag}\right) = \{\phi' \in \mathcal{L}^2\left(\Omega_{mag}\right), \mathbf{grad}\,\phi' \in \mathcal{L}^2\left(\Omega_{mag}\right), \phi'|_{\Gamma_\phi} = 0\} \tag{1.56}$$

with complementary boundaries $\Gamma_{\mathbf{B}}$ (for Neumann conditions) and Γ_ϕ (for Dirichlet conditions). The constitutive law is $\mathbf{B} = \mu_0\left(\mathbf{H} + \mathbf{M}\left(\mathbf{H}, \boldsymbol{\sigma}\right)\right)$ and the magnetic field is $\mathbf{H} = \mathbf{T} - \mathbf{grad}\,\phi$.

Finally, formulations based on the mechanical stress for elasticity are unusual and much more complex than displacement based formulations. This kind of formulation can be found, for example, in applications close to the incompressible limit, but has not been investigate yet for magneto-elastic coupling problems.

1.5.2 Integration, differentiation and inversion of simplified multiscale models

In order to enable the use of simplified multiscale models in device simulation tools, some important properties are detailed in this section. Integration of the model gives access to the energy stored in the material. Differentiation allows the application of differential time-stepping schemes and non-linear Newton-Raphson algorithms for the resolution. Finally, inverse models are needed for the implementation in the commonly used strain and magnetic flux density based formulations (such as the displacement and magnetic vector potential formulations).

For the sake of simplicity, the case of the numerical equivalent single crystal model is considered. All results can be straightforwardly extended to the equivalent simplified texture model by calculating mean values over the set of grain orientations. The case of the analytical model is not fully treated but its specificities, which come from its magnetic field dependent local magneto-elastic energy, are highlighted in a separate section.

1.5.2.1 Integration

The total magneto-elastic co-energy density w_{co} of an anhysteretic material can be defined as

$$w_{co} = \int \mathbf{B}.\mathrm{d}\mathbf{H} + \int \boldsymbol{\varepsilon} : \mathrm{d}\boldsymbol{\sigma} \tag{1.57}$$

where $\mathbf{B}$ and $\mathrm{d}\mathbf{H}$ are vectors, and $\boldsymbol{\varepsilon}$ and $\mathrm{d}\boldsymbol{\sigma}$ are second rank tensors. The integrals on $\mathbf{H}$ and $\boldsymbol{\sigma}$ are calculated between a reference state, which might be $(\mathbf{H} = \mathbf{0}, \boldsymbol{\sigma} = \mathbf{0})$, and the current state, independently of the path between these two states. The magnetic flux density is $\mathbf{B} = \mu_0(\mathbf{H} + \mathbf{M})$ and the total strain is $\boldsymbol{\varepsilon} = (\boldsymbol{\varepsilon}^e + \boldsymbol{\varepsilon}^\mu)$, where $\boldsymbol{\varepsilon}^e$ is the elastic strain tensor. The part of the co-energy

relative to the magneto-elastic behaviour is then

$$\int \mu_0 \mathbf{M}.\mathrm{d}\mathbf{H} + \int \boldsymbol{\varepsilon}^{\mu} : \mathrm{d}\boldsymbol{\sigma} = \frac{1}{A_s} ln \left(\sum_{\alpha} \exp\left(-A_s W_{\alpha}\right) \right) \tag{1.58}$$

which can be verified by partial differentiation with respect to the magnetic field or the mechanical stress. The co-energy can then be calculated for any loading from the energy associated with each domain family. It can be noticed that the total energy density *is not* the mean value of the energies associated with each domain family ($\sum_{\alpha} f_{\alpha} W_{\alpha}$), which means that the model implicitly includes interactions between domains. The energy density may be calculated from the co-energy density by

$$w = \mathbf{B}.\mathbf{H} + \boldsymbol{\varepsilon} : \boldsymbol{\sigma} - w_{co}. \tag{1.59}$$

1.5.2.2 Differentiation

Magnetisation ($\mathbf{M}$) and magnetostriction ($\boldsymbol{\varepsilon}$) can be differentiated with respect to the input variables, i.e. the magnetic field ($\mathbf{H}$) and the mechanical stress ($\boldsymbol{\sigma}$). The differential susceptibility tensor can be written as:

$$\frac{\partial \mathbf{M}}{\partial \mathbf{H}} = \sum_{\alpha} \mathbf{m}_{\alpha} \otimes \frac{\partial f_{\alpha}}{\partial \mathbf{H}} \tag{1.60}$$

because $\mathbf{m}_{\alpha}$ and $\boldsymbol{\alpha}$ do not depend on the magnetic field. It can be shown [14] that the partial derivative of f_{α} with respect to $\mathbf{H}$ is:

$$\frac{\partial f_{\alpha}}{\partial \mathbf{H}} = A_s f_{\alpha} \left(\left(\sum_{\alpha} f_{\alpha} \frac{\partial W_{\alpha}}{\partial \mathbf{H}} \right) - \frac{\partial W_{\alpha}}{\partial \mathbf{H}} \right) \tag{1.61}$$

From equation (1.17) to (1.20), and considering that the anisotropy energy does not depend on magnetic field and stress:

$$\frac{\partial W_{\alpha}}{\partial \mathbf{H}} = -\mu_0 \mathbf{m}_{\alpha} \tag{1.62}$$

Finally, the analytical expression for the differential susceptibility is obtained as:

$$\frac{\partial \mathbf{M}}{\partial \mathbf{H}} = \mu_0 A_s \left(\left(\sum_{\alpha} f_{\alpha} \mathbf{m}_{\alpha} \otimes \mathbf{m}_{\alpha} \right) - \mathbf{M} \otimes \mathbf{M} \right) \tag{1.63}$$

From equation (1.63), the differential susceptibility tensor appears to be proportional to the difference between the tensor product of the macroscopic magnetisation by itself and the volume fraction weighted average of the tensor product of the local magnetisation by itself. The other components of the differential model can be obtained in the same way:

$$\frac{\partial \boldsymbol{\varepsilon}^{\mu}}{\partial \boldsymbol{\sigma}} = A_s \left(\left(\sum_{\alpha} f_{\alpha} \boldsymbol{\varepsilon}_{\alpha}^{\mu} \otimes \boldsymbol{\varepsilon}_{\alpha}^{\mu} \right) - \boldsymbol{\varepsilon}^{\mu} \otimes \boldsymbol{\varepsilon}^{\mu} \right) \tag{1.64}$$

$$\frac{\partial \mathbf{M}}{\partial \boldsymbol{\sigma}} = A_s \left(\left(\sum_{\alpha} f_\alpha \mathbf{m}_\alpha \otimes \boldsymbol{\varepsilon}_\alpha^\mu \right) - \mathbf{M} \otimes \boldsymbol{\varepsilon}^\mu \right) \tag{1.65}$$

$$\frac{\partial \boldsymbol{\varepsilon}^\mu}{\partial \mathbf{H}} = \mu_0 A_s \left(\left(\sum_{\alpha} f_\alpha \boldsymbol{\varepsilon}_\alpha^\mu \otimes \mathbf{m}_\alpha \right) - \boldsymbol{\varepsilon}^\mu \otimes \mathbf{M} \right) \tag{1.66}$$

where $\frac{\partial \boldsymbol{\varepsilon}^\mu}{\partial \boldsymbol{\sigma}}$ is a fourth rank tensor, $\frac{\partial \mathbf{M}_{an}}{\partial \boldsymbol{\sigma}}$ and $\frac{\partial \boldsymbol{\varepsilon}^\mu}{\partial \mathbf{H}}$ are third rank tensors. The last two tensors verify $\mu_0 \left(\frac{\partial \mathbf{M}}{\partial \boldsymbol{\sigma}} \right)_{ijk} = \left(\frac{\partial \boldsymbol{\varepsilon}^\mu}{\partial \mathbf{H}} \right)_{jki}$ as they should, considering that they derive from the same co-energy and applying Schwarz theorem. The set of equations (1.63) to (1.66) constitutes the output of the differential simplified MSM.

1.5.2.3 Inversion

Full inversion of the model consists in allowing the magnetic flux density ($\mathbf{B}$) and the mechanical total strain ($\boldsymbol{\varepsilon}$) to be the input parameters (state variables) [16]. From the differential model, the inverse model can be obtained numerically. Using Voigt notation for the stress and strain tensors, the differential model can be written in matrix form as:

$$\begin{bmatrix} \mu_0 \mathrm{d}\mathbf{M} \\ \mathrm{d}\boldsymbol{\varepsilon}^\mu \end{bmatrix} = \begin{bmatrix} \mu_0 \frac{\partial \mathbf{M}}{\partial \mathbf{H}} & \mu_0 \frac{\partial \mathbf{M}}{\partial \boldsymbol{\sigma}} \\ \frac{\partial \boldsymbol{\varepsilon}^\mu}{\partial \mathbf{H}} & \frac{\partial \boldsymbol{\varepsilon}^\mu}{\partial \boldsymbol{\sigma}} \end{bmatrix} \begin{bmatrix} \mathrm{d}\mathbf{H} \\ \mathrm{d}\boldsymbol{\sigma} \end{bmatrix} = \boldsymbol{F} \begin{bmatrix} \mathrm{d}\mathbf{H} \\ \mathrm{d}\boldsymbol{\sigma} \end{bmatrix} \tag{1.67}$$

The inversion consists in finding $(\mathbf{H}, \boldsymbol{\sigma})$ such that:

$$\mathbf{B} = \mu_0 (\mathbf{H} + \mathbf{M}) \tag{1.68}$$

and

$$\boldsymbol{\varepsilon} = \mathcal{S} : \boldsymbol{\sigma} + \boldsymbol{\varepsilon}^\mu \tag{1.69}$$

where $\mathcal{S}$ represents the elastic compliance tensor ($\mathcal{S} = C^{-1}$). Using Newton-Raphson method, an approximate solution is found by solving iteratively:

$$\begin{bmatrix} \delta\mathbf{H} \\ \delta\boldsymbol{\sigma} \end{bmatrix} = -\boldsymbol{G}^{-1} \begin{bmatrix} \delta\mathbf{B} \\ \delta\boldsymbol{\varepsilon} \end{bmatrix} \tag{1.70}$$

where

$$\boldsymbol{G} = \begin{bmatrix} \mu_0 \boldsymbol{I} & 0 \\ 0 & \mathcal{S} \end{bmatrix} + \boldsymbol{F} \tag{1.71}$$

and $\begin{bmatrix} \delta\mathbf{B} \\ \delta\boldsymbol{\varepsilon} \end{bmatrix}$ is the residual. Some convergence properties of the simplified MSM inversion can be found in [16].

1.5.2.4 Inversion of the analytical SMSM

The magnetisation of the analytical SMSM can be differentiated with respect to the magnetic field from equation (1.49). The calculation of the full differential susceptibility tensor is relatively complex as shown in [16]. As the set of possible domain orientations follows the magnetic field and as only the diagonal components of the stress are considered in the associated basis, the local magneto-elastic energy depends on the applied magnetic field. The differentiation and integration of the analytical model are then more conveniently performed numerically. The inversion may also be performed using algorithms that do not need the evaluation of derivatives.

1.6 APPLICATIONS

1.6.1 Effect of mechanical stress on a Switched Reluctance Motor

A significant source of stress in electrical machines comes from assembling processes. Shrink-fitting method of the stator core into the motor frame and of the shaft into the rotor core generates a constant stress distribution that may impact the machine performance. As an example, considering a switched reluctance motor with a stator external diameter of $6.8\,cm$ and a shrink-fitting equivalent to a radial displacement of $2.5\,\mu m$, tangential tensile stress in the rotor and compressive stress in the stator can reach 20 MPa and -10 MPa, respectively (Fig. 1.8). Using an hysteretic Jiles-Atherton model including the multiscale approach as presented in section 1.2.2, and considering a pinning parameter depending on the domain configuration [14], the effect of stress on hysteresis loops and on losses can be quantified for any applied field (Fig. 1.9). Neglecting the stress induced by magnetostriction, the stress distribution obtained with an elastostatic formulation can be introduced in the magnetostatic formulation as a constant tensor parameter for the material constitutive model. This partially coupled magneto-mechanical approach allows quantifying the distribution of hysteresis losses for the device in operation (Fig. 1.10). The stress can locally change the hysteresis loss density by a factor of -60 to 80%. This results in a overall hysteresis loss increase of more than 5% [14].

1.6.2 Magnetostriction induced deformations in a transformer

Magnetostriction strain induces deformations of the magnetic core of transformers which may result in loud noise in operation. A three-phase transformer made of an alternate arrangement of grain-oriented (GO) silicon steel sheets can be analysed in two dimensions using homogenization techniques and a multiscale approach for the evaluation of the magnetostriction tensor distribution [17]. GO iron silicon presents strong magnetostriction strain (Fig. 1.11) and anisotropy which makes it sensitive to the local magnetic field intensity and direction. The distribution of magnetostriction strain can be calculated as a function of time (or

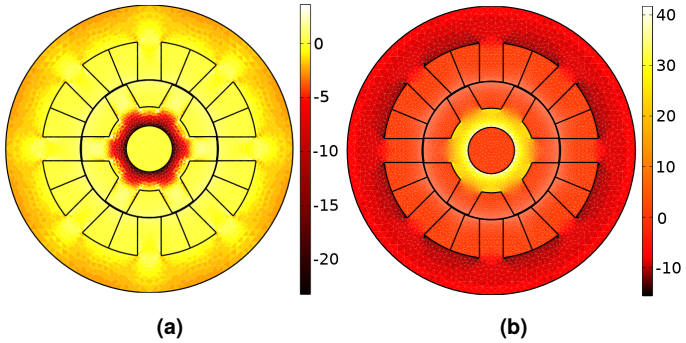


FIGURE 1.8 (a) radial and (b) tangential principal components of stress (MPa) from [14].

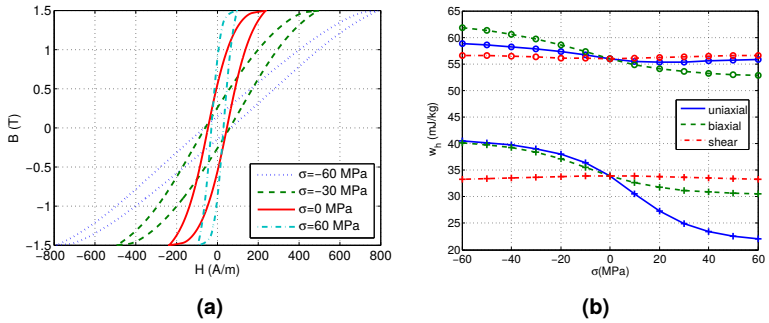


FIGURE 1.9 (a) hysteresis loops under unixial stress and (b) hysteresis loss density under uniaxial, biaxial and shear stress, for alternating (+) and circular (o) induction ($B_{max} = 1T$) from [14].

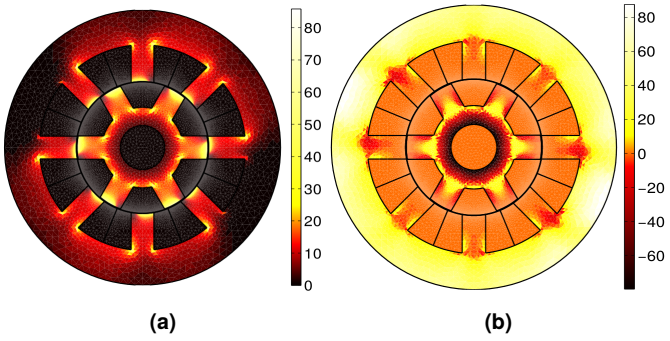


FIGURE 1.10 (a) distribution of hysteresis loss density and (b) relative difference between stressed and unstressed (reference) configurations (%) from [14].

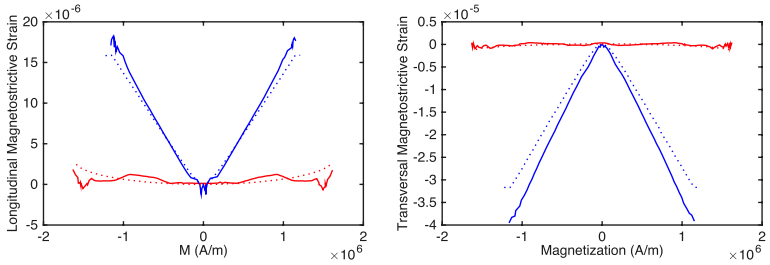


FIGURE 1.11 Parallel and transverse magnetostriction from MSM and experiment from [17].

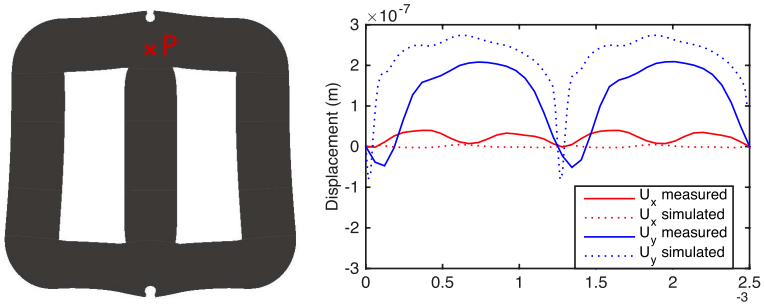


FIGURE 1.12 Simulated deformed core shape (scale factor of 2×10^4) for $200At$ in the central coil and displacement at point P as a function of time compared to measured displacement from [17].

applied current) using a magnetostatic formulation together with a multiscale homogenized model and neglecting other sources of stress. The induced total strain and the corresponding local displacement are computed in a second step using a dynamic elastic formulation with the distribution of magnetostriction strain as a source term. Local displacement obtained with this method compares well with experiments (Fig.1.12) and can be readily used for noise generation analysis.

1.7 CONCLUSION

This chapter was dedicated to the multiscale description of magnetic behaviour. From thermodynamic considerations at the local scale, it is possible to define a simplified modelling approach for magnetic single crystals, based on a statistical description of domain microstructure. For that purpose the single crystal is divided into domain families, each associated with an internal variable corresponding to its volume fraction. The evolution law of the internal variables is given by a Boltzmann-like relation. Polycrystalline materials are then treated as single crystals aggregates. The non-uniformity of magnetic field and stress is taken into account using scale transition rules derived from homogenization theory. Anhysteretic behaviour is first considered and hysteresis is then superim-

posed using two classical phenomenological approaches. In this chapter a focus has been made on the description of magneto-mechanical problems, namely the effect of stress on magnetisation and magnetostriction strain. A specific emphasis was given on the requirements in order to implement these magneto-mechanical constitutive equations into practical numerical tools for the design of electromagnetic devices. It is worth noting that the approach is intrinsically multiaxial and can naturally deal with any multiaxial stress state, whatever its relative orientation with respect to the magnetic field. This is a crucial advantage compared to many models used in computational magnetics that consider the stress as a scalar quantity, which disqualifies them to deal with most of practical electromagnetic devices.

The applicability of the proposed methodology is not restricted to the examples of magneto-elastic couplings presented in the chapter. It can be generalised to other types of phenomenon, many of which remain open research issues.

An interesting application is for instance the coupling between multiaxial stress and rotational magnetic field which is a great challenge for both modelling and experimental characterisation. The effects of plasticity on the magnetic behaviour of ferromagnetic materials is also a critical issue. A better understanding and description of the corresponding mechanisms and resulting behaviour would allow the prediction of the effect of forming and assembly processes on the nominal performance of electromagnetic devices. This is for example a great challenge for the optimisation of electrical machines. Multiscale approaches can be a great help in defining residual stresses related to these processes and estimating their consequences on the material behaviour.

The multiscale approach can also serve as a producer of tools for electrical engineers. A good example is the definition of equivalent stresses. The objective in that case is to define a fictitious uniaxial stress that has the same effect on the material - from a given perspective - as the real multiaxial stress state. Such an equivalence is of course not universal and different equivalences can be defined from the multiscale approach: equivalence in magneto-elastic energy, in macroscopic magnetisation, in magnetostriction, etc. It provides a simple tool for the quick assessment of a given external loading. Such approaches have been instrumental in Mechanics (see Von Mises or Tresca equivalent stress for the plasticity of metals or Rankine criterion for the fracture of ceramics) and can also meet many applications in computational electromagnetics.

ACKNOWLEDGEMENTS

In addition to the contributions by the authors, this chapter is largely based on the works of former PhD students R. Corcolle, K.J. Rizzo, M. Rekik, S. Lazreg, F.S. Mballa, M. Liu. We are grateful for their contribution.

Bibliography

[1] A.C. Eringen, G.A. Maugin. Electrodynamics of Contina.Springer, New York, 1990.

[2] A. Hubert, R. Schäfer. Magnetic Domains. The analysis of magnetic microstructures. Springer, 2008.

[3] W.F. Brown. Micromagnetics. John Wiley & Sons, New York, 1963.

[4] A. Aharoni. Introduction to the Theory of Ferromagnetism. Oxford University Press, New York, 1996.

[5] L. Néel, "Les lois de l'aimantation et de la subdivision en domaines élémentaires d'un monocristal de fer", J. Phys. Radiat., **5**:241-251, 1944.

[6] L. Daniel, O. Hubert, N. Buiron, R. Billardon, "Reversible magneto-elastic behavior: a multiscale approach", J. Mech. Phys. Solids, **56**:1018-1042, 2008.

[7] L. Daniel, M. Rekik, O. Hubert, "A multiscale model for magneto-elastic behaviour including hysteresis effects", Arch. Appl. Mech., **84(9)**:1307-1323, 2014.

[8] T. Mura. Micromechanics of Defects in Solids. Martinus Nijhoff Publishers, Dordrecht, MA, 1982.

[9] R. Corcolle, L. Daniel, F. Bouillault, "Generic formalism for homogenization of coupled behaviors :application to magnetoelectroelastic behavior", Phys. Rev. B, **78(21)**: 214110, 2008.

[10] G. Bertotti, Hysteresis in Magnetism For Physicists, Materials Scientists, and Engineers. Academic Press, 1998.

[11] H. Hauser, "Energetic model of ferromagnetic hysteresis:Isotropic magnetization", J. Appl. Phys., **96(5)**: 2753–2767, 2004.

[12] D.C. Jiles, D.L. Atherton, "Theory of ferromagnetic hysteresis", J. Appl. Phys., **55(6)**: 2115-2120, 1984.

[13] A. J. Bergqvist, "A simple vector generalization of the Jiles-Atherton model of hysteresis", IEEE Trans. Magn., **32(5)**:4213-4215, 1996.

[14] L. Bernard, L. Daniel, "Effect of stress on magnetic hysteresis losses in a switched reluctance motor: application to stator and rotor shrinking fitting", IEEE Trans. Magn., **51(9)**: 7002513, 2015.

[15] M. Rekik, "Mesure et modélisation du comportement magnéto-mécanique dissipatif des matériaux ferromagnétiques à haute limite élastique sous chargement multiaxial", PhD thesis (in French), Ecole normale supérieure de Cachan, France, 2014.

[16] L. Bernard, B.J. Mailhé, N. Sadowski, N.J. Batistela, L. Daniel, "Multiscale approaches for magnetoelasticity in device simulation", J. Magn. Magn. Mater., **487**:165241, 2019.

[17] M. Liu, O. Hubert, X. Mininger, F. Bouillault, L. Bernard, "Homogenized Magnetoelastic Behavior Model for the Computation of Strain Due to Magnetostriction in Transformers", IEEE Trans. Magn., **52(2)**:8000212, 2016.

[18] A. Bossavit, "Bulk forces and interface forces in assemblies of magnetized pieces of matter", IEEE Trans. Magn., **52(3)**:7003504, 2016.